A PROGRAM FOR NUMERICAL CALCULATION OF DYNAMIC STRESS-STRAIN STATE AND STRENGTH OF HOLLOW MULTILAYER ANISOTROPIC CYLINDERS AND SPHERES. PART 2. COMPARISON OF NUMERICAL RESULTS WITH EXPERIMENTAL AND THEORETICAL FOR CYLINDERS

P. P. Lepikhin, V. A. Romashchenko, O. S. Beiner,   UDC 539.3

V. N. Storozhuk, Yu. N. Babich, and E. V. Bakhtina

A comparison of the numerical results, which are obtained using the application software package developed at the Pisarenko Institute of Problems of Strength under the National Academy of Sciences of Ukraine for the calculation of stress-strain state and strength of multilayer composite cylinders and spheres under internal pulse loading, with the known theoretical and experimental data for a number of composite and metal-composite cylinders under internal axisymmetric explosion.

Keywords: composite materials, explosive, numerical methods, multilayer cylinder, stress-strain state, strength.

A brief description of the application software package (ASP) developed at the Pisarenko Institute of Problems of Strength under the National Academy of Sciences of Ukraine, which makes it possible to determine the stress-strain state (SSS) and strength of multilayer composite cylinders (generally with spiral orthotropic layers) of finite length with different boundary conditions at ends and spherically transtropic spheres under internal explosive loading, was presented earlier in [1].

The developed ASP is tested [2] regarding SSS of cylinders. Moreover, a comparison of numerical data (due to the lack of solution for dynamic statements) with some results of the solution of static linear elastic problems at small displacements and strains obtained both analytically and numerical-analytically has been made. The calculation results are compared with the experimental data for composites reinforced with fibers [3,4], which are numerical for shell approximation [5], as well as with that data obtained using a commercial package LS-DYNA.

The purpose of the present paper lies in the comparison of numerical solutions obtained using the developed ASP with the known numerical and experimental data by SSS and strength of multilayer composite and metal-composite cylinders with free ends under internal axisymmetric pulse loading initiated by blasting of an explosive charge (EC) at the center of shell symmetry.

The experimental and numerical data for performing a comparative analysis were taken from references. Multilayer cylinders from unidirectional reinforced composite materials (CM), each layer of which can be described using transtropic elastic material, or metal-composite cylinders with internal metallic layer additional to the layers from CM were investigated in all the considered papers. The direction of reinforcement of CM layers or composite part of metal-composite is circumferential (±90°), axial (0) or spiral with one or the other angle of reinforcement φ not equal to 0 and ±90°. Such structures as it follows from [3, 6] have a number of advantages compared to the cylinders from CM reinforced with fibers. Let us consider several variants of comparison.

Variant 1. The paper [7] presents the experimental investigation of dynamic response and strength of composite shells of four types with different schemes of reinforcement under internal explosive loading. Thus the maximum annular strains on the external surface (ε_1 – in the central section and ε_2 – in the section at a distance of 100 mm away from the central one) and the period T of the fundamental period of radial vibrations were determined. The shell state with or without the presence of visible macrofracture in the finite deformed state is described.

For the numerical investigation a shell [7] with a more complete set of data required for the calculation with a winding convenient for comparison ($\varphi = 90°$) is selected, when the number of layers does not play any role. In [7] also no specific geometric dimensions are set for the cylindrical shell under study, however, there are values for the mass of charge $m_{ch} = 0.134$ kg, the thickness ratio of the shell wall $100H/R_{in} = 9.95\%$, the parameter $\xi = M_{TNT}/M = 7.7 \cdot 10^{-3}$ and the average density of the shell material $\rho = 1880$ kg/m^3, where H is the thickness of the shell wall, R_{in} is its internal radius, M is the shell mass of length of $4R_{in}$, and M_{TNT} is the TNT-equivalent explosive mass. This makes it possible to calculate the required geometric dimensions of the shell: $R_{in} = 0.152$ m, $H = 0.015$ m, external radius $R_{ex} = 0.167$ m, and length $L = 4R_{in} = 0.608$ m. The cylinder is manufactured by coiling the cloth (made of glass fibers of VMPS class) on the technological fixture (ÉDT-10 class). The TNT-equivalent mass of explosive charge M_{TNT} is 0.15142 kg determined using the procedure described in [8]. The explosive was in the center of the shell.

In [7] by the method [9] using the physical and mechanical characteristics of glass fiber, binder and volumetric content of glass fiber in the material ϑ_f [7, 10] the elastic characteristics of CM were calculated (Table 1). Here, ϑ_f is determined from the formula:

$$\rho = \rho_f \vartheta_f + \rho_m (1 - \vartheta_f),$$

where ρ is the density of CM (glass fiber), $\rho_f = 2540$ kg/m^3, $\rho_m = 1230$ kg/m^3 is the density of glass fiber and epoxy resin (matrix), respectively [10]. For the case considered $\vartheta_f = 0.496$.

To carry out the numerical calculations for the transtropic material meeting all the criteria of strength in ASP it is required additionally to determine the moduli of elasticity and shear and Poisson's ratio as well as the ultimate strength and ultimate strains in tension, compression along the main axes of anisotropy and shear in the principal planes of the material. The procedure described in [9] does not make it possible to do it.

To determine these characteristics of the material, the missing constants of CM (both elastic and strength) are calculated knowing the specific weight of fibers and composite density as well as the reference data for main mechanical characteristics of glass fiber VMPS and binder ÉDT-10 [7, 10] based on the chosen analytical methods [11], namely: mixture rule and CCA (composite cylinder assemblage) that are simulate the mechanical characteristics of glass composites most accurately. Table 1 presents the mechanical characteristics of the material obtained from the calculation.

The following symbols are taken in Table 1 and below: E, E' are the Young moduli in the plane of isotropy and in the fiber direction, respectively, G' is the shear modulus in the plane parallel to fibers, ν, ν' are the Poisson's ratios in the plane of isotropy and in the plane parallel to fibers, σ'_t, σ'_c are the tensile and compression strength in the fiber direction, τ' is the shear strength in the plane parallel to fibers, τ is the shear strength in the isotropy plane, ε'_t, ε'_c are the ultimate tensile and compression strains in the direction of fibers, ε_t, ε_c are tensile and compression strains in the isotropy plane, and γ', γ is the ultimate shear strains in the plane parallel to fibers and in the isotropy plane, respectively.

The ultimate strain values ε'_t, ε'_c, ε_t, ε_c, γ', and γ are determined using the ultimate stress values and the Hook law for the transtropic body [2].

The following parameters were taken considering the data for the numerical calculation presented in Table 1: $\rho = 1880$ kg/m^3, $E' = 37900$ MPa, $E = 8900$ MPa, $G' = 2840$ MPa, $\nu' = 0.28$, $\nu = 0.36$, $\sigma'_t = 1831$ MPa, $\sigma'_c = 634$ MPa, $\sigma_t = 36.75$ MPa, $\sigma_c = 193$ MPa, $\tau' = 63.1$ MPa, $\varepsilon'_t = 4.83\%$, $\varepsilon'_c = 1.67\%$, $\varepsilon_t = 0.41\%$, $\varepsilon_c = 2.14\%$, $\gamma' = 1.11\%$, $\gamma = 0.74\%$.

TABLE 1. Mechanical Characteristics of Fiber, Binder and CM VMPS/ÉDT-10

Mechanical characteristics	Fiber VMPS	Binder ÉDT-10	Calculation using the procedure [9]	Calculation using the procedures [11]
E', GPa	73	2.9	37.9	38.6
E, GPa	73	2.9	8.9	8.3
G', GPa	–	–	–	2.84
ν'	0.2	0.4	0.28	0.29
ν	–	–	–	0.36
σ'_t, MPa	3500	75	–	1831
σ'_c, MPa	1145	160	–	634
σ_t, MPa	–	–	–	36.75
σ_c, MPa	–	–	–	193
τ', MPa	–	51	–	63.1
ρ, g/cm^3	2.54	1.23	1.88	1.9

TABLE 2. Comparative Analysis of Numerical and Experimental Data

Calculation	ε_1, %	ε_2, %	T, μs	$\dot{\varepsilon}$, s^{-1}
Developed ASP	$\dfrac{1.15}{0.95}$	$\dfrac{0.6}{0.5}$	$\dfrac{230}{227}$	$\dfrac{150}{165}$
LS-DYNA	$\dfrac{1{,}14}{0{,}95}$	–	$\dfrac{211}{227}$	–

Note. Here and in Tables 4–7: the experimental results are given above the line, the numerical ones – below the line.

Strength characteristics of CM meet the condition of invariance in the isotropy plane as well as satisfy the required and sufficient conditions of stability for quadratic criteria of strength [2, 13].

Since the angle of winding of all the shell layers is the same (90°), in the calculations it was accepted that the cylinder is single-layered. Pulse pressure was determined using the same algorithm as LS-DYNA Load Blast in the commercial package LS-DYNA. This algorithm showed a high accuracy in the simulation during comparison with the experiments data [14]. A two-dimensional axisymmetric boundary problem was being solved. To evaluate the strength, strength criteria including maximum stresses, maximum strains, Hoffman and generalized von Mises criterion were used.

The comparison of experimental and numerical data was made using the maximum circumferential strain in two sections of the shell, the fundamental period of radial vibrations T and the maximum velocity of circumferential strain $\dot{\varepsilon}$ (Table 2). In accordance with the data [7] an error in determination of the specified magnitudes (as well as average density of CM) does not exceed 10%.

An error in the calculation results for ε_1, ε_2, $\dot{\varepsilon}$, and T is 21, 20, 9, and 1.3%, respectively.

Circumferential cracks were experimentally detected for the shell after loading on the external surface in the central section. Calculation also showed the exceeding of strength at some moments in this section by all the fracture criteria used in ASP.

Variant 2. The dynamic strength and deformability of cylindrical shells made of basalt plastic and basalt plastic with an internal layer made of low-carbon steel (metal-filled plastic) under single internal explosive loading were experimentally investigated in [15]. From the experimental results the following parameters were determined: the maximum circumferential tensile strain in the central section ε_1 and time of its achievement τ_1, the maximum circumferential compression strain in the central section $\bar{\varepsilon}_1$, the fundamental period of radial vibrations T and etc. The character of damage in the shell was also analyzed and its measurements were performed.

For the calculation the test 1 from Table 2 [15] was chosen. The composite shell with the following geometric parameters was investigated: $R_{in} = 0.075$ m, $H = 0.0067$ m, $R_{ex} = 0.0817$ m, $L = 4R_{in} = 0.3$ m, reinforcement angles $\varphi = 90°$ (circumferential reinforcement) and $\pm 35°$ with alternation of double annular layers and seven double spiral layers (thickness ratio 1:1). The shells made of basalt plastic RB9-1200/ÉDT-10 were tested, they are fabricated using the method of wet winding of composite basalt fibers with a subsequent thermal treatment required for the binder polymerization. The shell mass = 2.054 kg, during weighting an error did not exceed more than 1% [15]. The charge mass $M_{exp} = 0.0238$ kg ($M_{TNT} = 0.0269$ kg).

Their minimum, maximum and average values from the series of tests are stated for all experimentally determined mechanical characteristics of basalt plastic.

In current calculations the minimum values of mechanical characteristics were taken based on the following reasons:

(i) data in Tables 2 and 3 [15] contain the information on the shell geometry and its mass that enables one to calculate density of CM (2030 kg/m^3);

(ii) using the analytical procedures, which describe the properties of unidirectional fibrous CM made of glass-reinforced plastic [11], and knowing the density of CM, binder and fibers, the mass content (23%) of the binder was determined within the range of 14.45–23.24%, which is in [15] is for the specimens used in the experiments. Basalt plastic with a mass concentration of binder 23% virtually coincides with the specimen material [15] with the minimum elastic characteristics. The elastic and strength characteristics are used from [15] and are presented in SI in Table 1.

For numerical calculation it is required additionally to determine the shear modulus and Poisson's ratio in the plane perpendicular to the reinforcement plane (isotropy plane) as well as shear strength in the isotropy plane. To predict the elastic characteristics, CCA procedure was used. Shear strength τ in the isotropy plane was determined from the conditions of invariance for quadratic fracture criteria [2, 13]. Thus, for the generalized von Mises criteria it is 45.1 MPa, for Hoffman – 39.1 MPa. Since in the applications von Mises criteria are used more often than the Hoffman criteria, in the calculations using the criteria of maximum stresses and maximum strains $\tau = 45.1$ MPa was assumed.

In the numerical investigation of basalt plastic RB9-1200/ÉDT-10 the following parameters are taken: $\rho = 2030$ kg/m^3, $E' = 50{,}800$ MPa, $E = 13{,}900$ MPa, $G' = 5625$ MPa, $\nu' = 0.267$, $\nu = 0.35$, $\sigma'_t = 1097$ MPa, $\sigma'_c = 629$ MPa, $\sigma_t = 47.8$ MPa, $\sigma_c = 127.4$ MPa, $\tau' = 40.57$ MPa, $\tau = 45.1$ MPa, $\varepsilon'_t = 2.16\%$, $\varepsilon'_c = 1.24\%$, $\varepsilon_t = 0.34\%$, $\varepsilon_c = 0.92\%$, $\gamma' = 0.36\%$, and $\gamma = 0.44\%$.

For the selected fiber wound composite in [15] the exact amount of layers and order of their alternation is not stated. As it was mentioned before only the ratio of layer thickness with a different angle of winding is specified.

The analysis shows that in the numerical calculation of a large amount of thin layers and simulation of each layer separately the execution time can be significant. Thus from the standpoint of efficiency and accuracy it is important to find the possibility to replace the real (usually significant) amount of layers with its smaller amount together with the retention of the ratio between layer thickness and different angles of winding, and evaluate the influence of the arrangement of layers in a package on the calculation accuracy.

In the calculations (all variants), the dimensions of the discrete elements were determined from the condition of discretization of the smallest layer (along its thickness) using two elements along the thickness and the ratio between the element thickness and its width 1:2 that is further accepted. Let us note that the layer thickness with an angle of winding 90° is twice as large as the layer thickness with angles of winding 35 and −35°.

Table 3 presents the calculation results. The order of alternation of layers is from the internal to the external one along the cylinder thickness. For comparison the experimental value ε_1 from [15] is given. Moreover, for reinforcement schemes No. 1, 2, 3, and 4 the number of elements along the package thickness did not change (24), whereas along the thickness of the thinnest layers it equals to 6, 6, 3, and 2, respectively. For reinforcement scheme No. 2 below the line the calculation data are presented at the discretization of each thin layer using two elements along the thickness.

TABLE 3. Comparative Analysis of Numerical and Experimental Data for Different Reinforcement Schemes

No. of reinforcement schemes	φ, deg	ε_1, %
1	90/35/−35	1.850
2	35/−35/90	1.878 / 1.890
3	Two sets 35/−35/90	1.855
4	Three sets 35/−35/90	1.850
Experiment		2.200

TABLE 4. Comparative Analysis of Numerical and Experimental Data for Reinforcement Scheme No. 2

Material	ε_1, %	$\bar{\varepsilon}_1$, %	$\dot{\varepsilon}$, s^{-1}	τ_1, μs	T, μs
Basalt plastic 35/−35/90	1.878 / 2.200	1.66 / 1.10	673 / 597	41.0 / 45.1	123 / 123

TABLE 5. Comparative Analysis of Numerical and Experimental Data for Variant No. 3

Material	ε_1, %	$\bar{\varepsilon}_1$, %	$\dot{\varepsilon}$, s^{-1}	τ_1, μs	T, μs
Basalt plastic 35/−35/90	1.39 / 1.47	1.27 / 0.86	250 / 234	72.3 / 75.0	243 / 245

From Table 3 it is seen that the value closest to the experiment data is for the reinforcement scheme No. 2. Here the number of package sets of three layers with this reinforcement scheme influences the result feebly, whereas the execution time for No. 2 with a decrease of the number of elements in the layers 3×3 times decreases by 27 times.

Also the calculations for a single-layered cylinder with the reinforcement angles close to 90° were conducted. In the range of the reinforcement angle from 85–90° error in determination of circumferential strain does not exceed 0.8%, circumferential stresses – 1.6%. Thus the circumferential reinforcement angle is further accepted to be 90°.

Table 4 presents the results of comparison of the numerical and experimental results. In the calculation discretization using two elements along the thickness of the thinnest layer was used.

As it is seen from the data in Table 4, an accuracy of the numerical determination of the maximum circumferential tensile and compression strains as well as strain rate in the midsection and also the time for attainment of the maximum strain value is 14.6, 50.9, 12.7 and 9%, respectively. The discrepancy between the numerical and experimental data on the period of radial vibrations of the shell was not observed.

In the course of experiment on the internal surface of the shell delamination of the material with 1.2 mm in thickness [15] was detected. The calculation also showed that, in accordance with all fracture criteria used in ASP, at some instants of time strength in these parts of shell can be violated.

Variant 3. For the calculation the composite shells with the following parameters (test 1 from Table 3 [15]) were used: $R_{in} = 0.14775$ m, $R_{ex} = 0.16122$ m, $H = 0.01347$ m, $L = 0.6$ m, and $\varphi \approx 90$ and $\pm 35°$ with alternation of 14.5 double annular layers and 10 double spiral layers. The relative thickness values for the layers with different angles of winding correlate as 10:10:29. The mass of explosive charge $M_{exp} = 0.135$ kg ($M_{TNT} = 0.15255$ kg). The shell mass is 15.75 kg, i.e., density of CM equals to 2010 kg/m^3, the mass content of the binder is 24%, which is virtually consistent with the specimen material [15] with the minimum elastic characteristics. Therefore the same characteristics of basalt plastic as in Variant 2 were used in the calculations. As it is seen from Table 5 the discrepancy between the calculation and experimental results by ε_1, $\bar{\varepsilon}_1$, $\dot{\varepsilon}$, τ_1, and T is 5.44, 47.7, 6.8, 3.6, and 0.8%, respectively.

TABLE 6. Comparative Analysis of Numerical and Experimental Data for Variant No. 4

Metal-composite	ε_1, %	$\bar{\varepsilon}_1$, %	τ_1, μs	$\dot{\varepsilon}$, s^{-1}
Basalt plastic	$\dfrac{1.73}{1.72}$	$\dfrac{1.30}{0.86}$	$\dfrac{45.0}{42.1}$	$\dfrac{544}{592}$
St. 3 steel (35/−35/90)				

The experiments showed that shells did not exhibit any visible damages. The calculations using the maximum stresses and strains criteria, as well as the Hofman criteria, provide evidence of the strength violation, since using the generalized von Mises criterion it does not exceed the ultimate value (unit).

Variant 4. The metal-composite shell with the following parameters was considered: $R_{in} = 0.07501$ m, $R_{ex} = 0.0818$ m, $H = 0.00679$ m, and $L = 4R_{in} = 0.3$ m. The shell made of low-carbon steel with thickness of 1 mm was inserted inside the basalt plastic shell. The shell was obtained by rolling the sheet to cylinder and by butt welding. The steel grade in [15] is not specified. At the same place it is noted that the chosen external diameter of steel shell provides the minimum gap regarding the internal diameter of the basalt plastic shell. The gap size is also not specified here. The scheme of reinforcement of the shell basalt plastic part is the alternation of double spiral layers with an angle of reinforcement $\varphi = \pm 35°$ and annular layer $\varphi = 90°$ with an angle at the thickness ratio 1:1:2. The material of the shell composite part is basalt plastic RB9-1200/ÉDT-10. The total mass of the shell is 3.135 kg, the mass of the steel part of the shell is 1.099 kg, the composite part mass is 2.036 kg, i.e., density of CM is 2.03 kg/m^3, the mass content of the binder is 22.9%, which is virtually consistent with the specimen material [15] with the minimum elastic characteristics. Therefore the same characteristics of basalt plastic as in Variant 2 were used in the calculations. The charge mass $M_{TNT} = 0.034$ kg. The St. 3 steel with the following characteristics was used as the steel shell material: $\rho = 7830$ kg/m^3, $E = 202{,}000$ MPa, $\nu = 0.3$, and yield stress $\sigma_Y = 210$ MPa [16].

The cylinder underwent discretization using the elements by layers in the thickness direction from the internal to external into 4/5/5/14 cells.

Table 6 presents the results of calculations and experiments.

An error in determination of the maximum circumferential tensile and compression strains, time of attainment of the maximum strain, and strain rate is 0.5, 51.2, 6.8, and 8.1%, respectively.

Significant residual plastic strains of the internal steel cylinder took place for the shell in question [15], which was different also in the calculations. Moreover, CM strength was violated in accordance with the all fracture criteria used.

Variant 5. In paper [17] deformation and fracture of glass-plastic shells were experimentally investigated. The wound cylinders had a combined scheme of reinforcement with alternation of double spiral ($\varphi = \pm 45°$) and annular ($\varphi = 90°$) layers with the thickness ratio 1:1:2. In the course of investigation the specimens were measured and weighted. As a result of the experiments the maximum circumferential strain ε_1, the maximum circumferential strain rate $\dot{\varepsilon}$, and fundamental periods of radial and axial vibrations were determined. The shell also has the following geometric dimensions: $R_{in} = 0.15$ m, $H = 0.00736$ m, and $L = 4R_{in} = 0.6$ m. The shell material is glass-plastic RVMN-10-1260-80/ÉDT-10, whose experimentally determined characteristics were taken from [15, 17]: $\rho = 1979$ kg/m^3, $E' = 53{,}900$ MPa, $E = 8860$ MPa, $G' = 4978$ MPa, $\nu' = 0.276$, $\nu = 0.353$, $\sigma'_t = 1470$ MPa, $\sigma'_c = 389$ MPa, $\sigma_t = 26.2$ MPa, $\sigma_c = 70.5$ MPa, $\tau' = 35$ MPa, $\tau = 24.8$ MPa (by the Hofman 21.5 MPa), $\varepsilon'_t = 2.73\%$, $\varepsilon'_c = 0.72\%$, $\varepsilon_t = 0.3\%$, $\varepsilon_c = 0.8\%$, $\gamma' = 0.35\%$, and $\gamma = 0.38\%$. Moreover, the data missing in [15, 17] are determined the same way as in Variant 1. Discretization is used along the thickness by the layers from the internal to external one (4/4/8 cells).

Table 7 presents the calculation and experimental results.

The comparison of the calculation and experimental data of the maximum circumferential tensile strain and strain rate provides evidence of the fact that the difference between them is 24 and 6.5%, respectively, the calculation of the fundamental period of radial and axial vibrations is within the range of the corresponding periods for a number of similar experimentally investigated shells.

Table 7. Comparative Analysis of Numerical and Experimental Data for Variant No. 5

Material	ε_1, %	T, µs	$\overline{T}$, µs	$\dot{\varepsilon}$, s^{-1}
Glass-plastic PBMN with a scheme of reinforcement 45/–45/90	$\dfrac{0.56}{0.45}$	$\dfrac{225}{215-245}$	$\dfrac{461}{450-495}$	$\dfrac{115}{108}$

Note. $\overline{T}$ is the fundamental period of axial vibrations.

TABLE 8. Comparative Analysis of Numerical and Experimental Data for Variant No. 6

Data acquisition	ε_1, %	τ_1, µs	T, µs
Experiment	1.470	75.0	245
Calculation [18]	1.290 (13.0)	74.0 (1.3)	249 (1.6)
ASP calculation	1.369 (6.87)	76.0 (1.3)	246 (0.4)

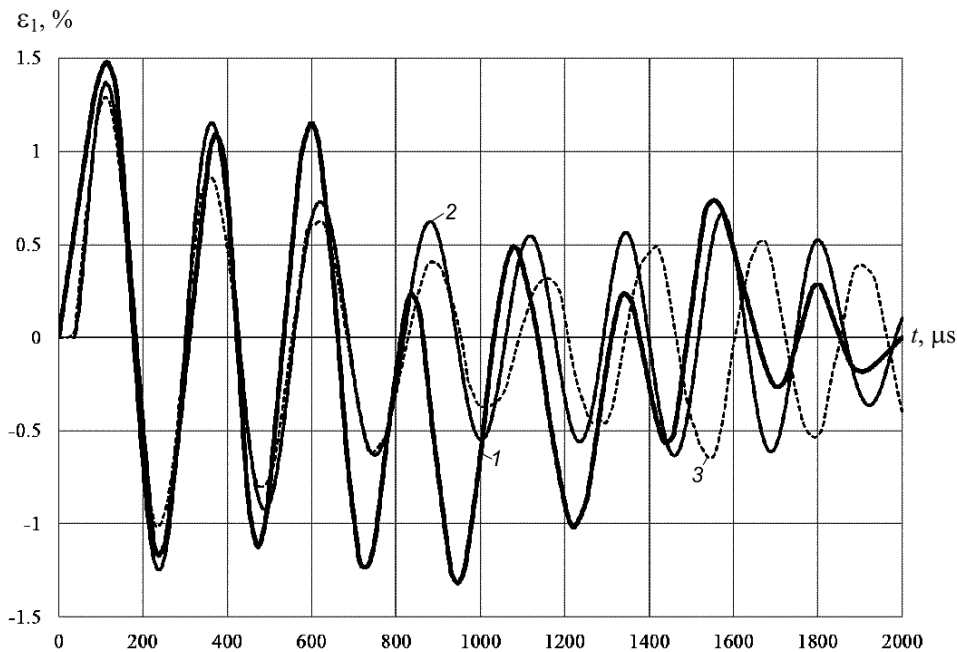**Note.** An error is given in brackets (in %).

Fig. 1. Variation of the circumferential strain of the external surface of cylinder in the midsection in time: (*1*) experimental data, (*2*) APS, (*3*) [18].

In the course of experiment no visible damages in the shell under study were detected, while the results of calculations showed that the strength condition was violated by all fracture criteria used in ASP.

Let us note that the charges with the minimum mass were used in the selected experiments. Here the minimum values ε_1, lack of fractures in accordance with the estimates [15] and one of the largest set of experimental data for comparison were used. Small values ε_1 practically do not lead to significant fracture in the material and, consequently, to the variation of its properties during deformation. It follows thence that there are small errors in the numerical determination of SSS and strength using the developed ASP, in which CM properties do not change during deformation. This mainly refers to the first quarter of the vibration mode. The calculations of the maximum circumferential strain on the external surface of the shell at the location of charge showed that the discrepancy with the experiment does not exceed 24%. Moreover, in the numerical calculation the shell is more rigid, since the variation of the material properties during fracture in the process of deformation is not considered. The other situation is observed during the material compression. The discrepancy between the results by $\overline{\varepsilon}_1$ is quite significant, which is caused particularly by the material fracture.

Variant 6. In [18], the numerical calculation was performed using the package LS-DYNA for the basalt plastic shell similar in geometry to the material and loading conditions of the shell from [15] (test 1 from Table 3) based on the comparison with the experimental data. The shell dimensions, ratio between thicknesses of the reinforced layers, angles of reinforcement and order of their arrangement were specified. The physical and mechanical characteristics of basalt plastic are not given. The characteristics of basalt plastic RB9-1200/ÉDT-10 required in the developed APS were taken from Variant 3, where the calculations were conducted for test 1 from Table 3 [15]: $\rho = 2030 \text{ kg/m}^3$, $E' = 50{,}800$ MPa, $E = 13{,}900$ MPa, $G' = 5625$ MPa, $\nu' = 0.267$, $\nu = 0.35$, $\sigma'_t = 1097$ MPa, $\sigma'_c = 629$ MPa, $\sigma_t = 47.8$ MPa, $\sigma_c = 127.4$ MPa, $\tau' = 40.57$ MPa, $\tau = 45.1$ MPa, $\varepsilon'_t = 2.16\%$, $\varepsilon'_c = 1.24\%$, $\varepsilon_t = 0.34\%$, $\varepsilon_c = 0.92\%$, $\gamma' = 0.36\%$, and $\gamma = 0.44\%$.

The shells with the following geometric dimensions and parameters of reinforcement were investigated: $R_{ex} = 0.16122$ м, $L = 0.6$ m, and $H = 0.01347$ m. The angles of reinforcement of layers 35/−35/90 with thicknesses of 3.8/3.8/5.9 mm from internal layer to external one, respectively, and $M_{TNT} = 0.135$ kg.

The maximum circumferential strain in central section, time of its attainment and fundamental period of radial vibrations were determined using the calculation results. Table 8 and Fig. 1 present the comparison of theoretical and experimental results.

The calculations showed that the conditions of strength were violated by all fracture criteria under study.

CONCLUSIONS

1. The results of numerical calculations using the APS developed at the Pisarenko Institute of Problems of Strength under the National Academy of Sciences of Ukraine aimed at determination of SSS at the first quarter of vibration period of the shell are in good correlation with the known experimental and numerical data for all six calculation variants. An error in determination of the maximum circumferential tensile strain of the external surface of central section of the shell does not exceed 24%, for the time of its attainment – 9%, for the maximum circumferential strain rate of the points on the external surface of the shell central section – 12.7%, for the fundamental period of radial vibrations – 1.3%. Moreover, the experimental values are always larger than the theoretical ones. This provides evidence of the adequacy of replace of real wound composite with continuous transtropic medium, which indirectly confirm the conclusions on the accuracy of prediction using the analytical relations of the mechanical and strength properties of glass composites and basalt plastic selected in [11], which are investigated in this paper, as well as small errors in the experimental determination of the mechanical and strength properties of the materials. Since the known fracture criteria, including those ones used in ASP, are based on SSS, a high accuracy in the determination of SSS in ASP makes it possible to simulate this process well (with an adequate description using this or that initial fracture criteria).

2. Due to the calculation of the maximum circumferential compression strain at the second half-period of radial vibrations of the shell a significant error is obtained regarding the known experimental data. The maximum value of this error is 51.2%. This is caused by the fact that fracture in composite in accordance with the all fracture criteria used took place for all the calculation variants using ASP. This led to the fact that the real material of the shell, at least with the time of attainment of the maximum circumferential tensile strain for the external surface of central section of the shell at the first half-period of ultimate magnitude, was under service with a subsequent deformation even in fractured state, its continuity was violated, the mechanical characteristics varied. In reality the material was less rigid other than in the calculation. In all cases the experimental values of the maximum circumferential tensile strain on the external surface of central section of the shell were higher than the numerical ones.

3. The possibility to replace the real multi-layer composite with a multi-layer medium with the minimum number of layers with compliance of the thickness ratio of layers with this or other angle of winding and feeble influence on the accuracy in the calculation results of the order of layer arrangement in a package were numerically determined.

4. The efficiency of the initial fracture criteria for a three-axial SSS used in ASP was shown. At the same time, the data on shell fracture (presence of, at least, one visible macrocrack in the shell) used in the experiments do

not make it possible to determine the fracture initiation experimentally. Thus the comparison of the theoretical and experimental data on the initial fracture was not performed. The theoretically analyzed experimental investigations enable one to determine fracture visually at the end of deformation. It can be simulated numerically using the models of progressive fracture.

5. The numerical calculations demonstrate the fact that there is an insignificant discrepancy between the values of vibration period determined from the instant of initiation of deformation in a quarter and half of the period since the beginning (error does not exceed 4%).

REFERENCES

1. P. P. Lepikhin, V. A. Romashchenko, O. S. Beiner, et al., "A program for numerical calculation of dynamic stress-strain state and strength of hollow multilayer anisotropic cylinders and spheres. Part 1. Program description," *Strength Mater.*, **47**, No. 2, 249–256 (2015).

2. P. P. Lepikhin and V. A. Romashchenko, *Strength of Nonuniform Anisotropic Hollow Cylinders under Pulse Loading* [in Russian], Naukova Dumka, Kiev (2014).

3. A. G. Fedorenko, M. A. Syrunin, and A. G. Ivanov, "Criterion for selecting composite materials for explosion containment structures (review)," *Fiz. Goren. Vzryv.*, No. 5, 3–13 (2005).

4. A. G. Fedorenko, M. A. Syrunin, and A. G. Ivanov, "Influence of reinforcement structure in fiberglass on the strength of annular cylindrical shells," *Mekh. Kompoz. Mater.*, No. 4, 631–640 (1991).

5. N. A. Abrosimov, A. V. Elesin, "Numerical analysis of the influence of reinforcement structure on the dynamic behavior of composite cylindrical shells under explosive loading," *Probl. Prochn. Plast.*, No. 74, 78–83 (2012).

6. V. A. Romashchenko, Yu. N. Babich, and E. V. Bakhtina, "Strength assessment for composite and metal-composite cylinders under pulse loading. Part 2. Numerical evaluation of strength for multilayer cylinders of finite length under internal explosion," *Strength Mater.*, **44**, No. 5, 502–511 (2012).

7. M. A. Syrunin, A. G. Fedorenko, and A. T. Shitov, "Strength of cylinder shells made of glass plastic of different structure under explosive loading," *Fiz. Goren. Vzryv.*, No. 4, 108–115 (1989).

8. L. P. Orlenko, *Physics of Explosion and Impact. Textbook for Universities* [in Russian], Fizmatlit, Moscow (2006).

9. *Designing, Calculation, and Testing of Structures Made of Composite Materials* [in Russian], Issue 1, Zhukovskii Central Aerohydrodynamic Institute, Moscow (1973).

10. G. N. Gunyaev, *Structure and Properties of Polymer Fibrous Composites* [in Russian], Khimiya, Moscow (1981).

11. A. V. Bakhtina, "Selection of analytical methods for determination of mechanical characteristics of unidirectional composites based on glass fibers," *Strength Mater.*, **46**, No. 1, 64–70 (2012).

12. S. G. Lekhnitskii, *Theory of Elasticity of Anisotropic Body* [in Russian], Nauka, Moscow (1977).

13. P. P. Lepikhin and V. A. Romashchenko, "Methods and findings of stress-strain state and strength analyses of multilayer thick-walled anisotropic cylinders under dynamic loading (review). Part 3. Phenomenological strength criteria," *Strength Mater.*, **45**, No. 3, 271–283 (2013).

14. K. Spranghers, I. Vasilakos, D. Lecompte, et al., "Numerical simulation and experimental validation of the dynamic response of aluminum plates under free air explosions," *Int. J. Impact Eng.*, **54**, 83–95 (2013).

15. V. N. Rusak, A. G. Fedorenko, M. A. Syrunin, et al., "Limiting deformability and strength of basalt plastic shells under internal explosive loading," *Prikl. Mekh. Tekhn. Fiz.*, No. 1, 186–195 (2002).

16. G. S. Pisarenko, A. P. Yakovlev, and V. V. Matveev, *A Handbook of Materials Strength* [in Russian], Delta, Kiev (2008).

17. M. A. Syrunin, A. G. Fedorenko, and A. G. Ivanov, "Dynamic strength of cylindrical shells made of glass plastic under multiple explosive loading," *Fiz. Goren. Vzryv.*, No. 6, 102–107 (1997).

18. S. Nelson, "Explosive testing of open cylinders for verification of composite properties used in computational analysis," in: ASME 2012 Verification and Validation Symposium (May 2–4, 2012), Las Vegas, NV (2012).